Giant magnetostriction of $Fe_{1-x}Be_x$ alloy: A first-principles study

Soon Cheol Hong* and Won Seok Yun
Department of Physics, University of Ulsan, Ulsan 680-749, Republic of Korea

Ruqian Wu†
Department of Physics, University of California–Irvine, Irvine, California 92697-4575, USA

(Received 11 August 2008; revised manuscript received 21 January 2009; published 18 February 2009)

Magnetostriction coefficients of ordered BeFe alloys were investigated, using the first-principles full-potential linearized augmented plane-wave method. A giant magnetostriction coefficient (~1060 ppm) was predicted in the $Fe_{0.8125}Be_{0.1875}$ alloy. We elucidated the origin of giant magnetostriction coefficient in terms of electronic structures and their responses to the tetragonal lattice distortion.

DOI: 10.1103/PhysRevB.79.054419 PACS number(s): 75.80.+q, 71.20.Be, 75.30.Gw, 75.50.Bb

I. INTRODUCTION

Magnetostrictive materials are widely used in transducers, actuators, and sensors[1,2] and have attracted extensive attention in the last 50 years. Among them, rare-earth-based alloys such as Terfenol-D are considered to be the most successful category due to their large tetragonal magnetostrictive coefficients, $\lambda_{111} > 1000$ ppm (10^{-6}). However, these alloys are brittle, expensive, and require high magnetic field for saturation. Extensive investigations have been performed recently to seek innovative alloys, which may circumvent these drawbacks. Intriguingly, Clark and co-workers[3–6] found that iron-based alloys with Al, Be, and Ga have much enhanced magnetostriction (λ_{001} ~100–500 ppm) compared to pure bulk Fe ($\lambda_{001}=20$ ppm; $\lambda_{111}=-16$ ppm). This opens a new vista of achieving strong magnetostriction in ductile metallic materials, essential toward the design of excellent devices for a wide range of applications. Nonetheless, the mechanism of such an extraordinary enhancement of λ_{001} is still elusive,[7] which hinders further developments of new functional materials with even stronger magnetostriction. Two models have been proposed for the explanation of giant magnetostriction of FeGa alloys: either the intrinsic model that stems from impurity-induced electronic structure changes,[8,9] or the extrinsic one that relies on reorientation of precipitations under external magnetic field.[10] In both cases, the local atomic ordering is crucial for the determination of magnetostriction.[8,9,11,12] It is possible that both the intrinsic and extrinsic origins are important for the understanding of the magnetostriction of Fe-based alloys, especially in samples with high impurity concentrations.

The measured magnetostriction depends sensitively on thermal history,[13] indicating that the enhanced λ_{001} may result from metastable geometries. At the present stage, it is clear that the minority atoms tend to avoid forming first neighborhoods, but the pattern of their arrangement as second neighbor remains unknown. In our previous studies for ordered $Fe_{0.75}Ga_{0.25}$ alloy, we inspected three different simple crystal structures: $D0_3$, $L1_2$, and $L6_0$. The magnetoelasticity was found to be surprisingly sensitive to the change in local arrangement of atoms and the $B2$-like crystal structure, $L6_0$, was identified as the key one that contributes to positive magnetostriction. The $L6_0$ structure is strongly anisotropic and is unstable under tetragonal distortion,[14] which might be the origin of the drastic decrease in the tetragonal elastic modulus of $Fe_{1-x}Ga_x$ around $x \sim 0.25$, as observed by Clark and co-workers.[15,16]

Therefore, it is crucial to elucidate how the presence of nonmagnetic elements enhances the magnetostriction of Fe through modern density-functional calculations. In this study we focused on the intrinsic mechanisms that produce large magnetostriction in $Fe_{1-x}Be_x$ binary alloys. While the search for most probable atomic structures for random alloys is still a challenging issue in this field, it is equally important to identify appropriate local structures that produce high magnetostriction. Interestingly, with a set of structural models, we found that giant magnetostrictive coefficients of up to ~1000 ppm are attainable in $Fe_{1-x}Be_x$ alloys around $x \sim 0.18$. This important finding lays a foundation for further theoretical studies in this context and also motivates experimental investigations for the quest of superb magnetostrictive materials.

II. METHODOLOGY AND COMPUTATIONAL DETAILS

In the present calculations, we used a 16-atom unit cell and placed Fe and Be atoms in the bcc lattices, as shown in Fig. 1, for (a) $Fe_{0.9375}Be_{0.0625}$, (b) $Fe_{0.875}Be_{0.125}$, (c) $Fe_{0.8125}Be_{0.1875}$, and (d) $Fe_{0.75}Be_{0.25}$. These models reserve the cubic symmetry and are stable under tetragonal distortions.

The all-electron full-potential linearized augmented plane-wave (FLAPW) method[17,18] was used to solve the density-functional Kohn-Sham equations at the level of the generalized gradient approximation.[19] Augmented plane waves with an energy cutoff of 12.25 Ry (256 Ry) were used to expand the bases (charge and potential) in the interstitial region, while spherical harmonics with a maximum angular momentum of $l_{max}=8$ were used for expansions in the muffin-tin (MT) spheres ($r_{Fe}=2.2$ a.u. and $r_{Be}=2.0$ a.u.). To ensure the numerical convergence, we used 1183 k points to sample the irreducible Brillouin zone. The self-consistency was assumed when the root-mean-square differences between the input and output charge and spin densities are less than 3.0×10^{-5} $e/(\text{a.u.})^3$.

The spin-orbit coupling (SOC) term in the Hamiltonian for the valence states, H^{SOC}, was treated as a perturbation in

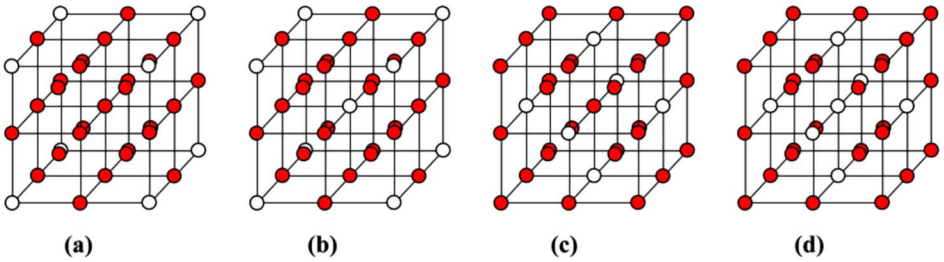

FIG. 1. (Color online) Unit cells used for (a) $Fe_{0.9375}Be_{0.0625}$, (b) $Fe_{0.875}Be_{0.125}$, (c) $Fe_{0.8125}Be_{0.1875}$, and (d) $Fe_{0.75}Be_{0.25}$. Dark balls are for Fe and white balls are for Be.

the second variational method, whereas the Dirac equation was solved for the core states. The torque approach was adopted for the determination of the strain dependence of magnetocrystalline anisotropy (MCA) energy (E_{MCA}). The magnetostrictive coefficients λ_{001} were obtained from calculating E_{tot} and E_{MCA} as functions of the lattice size along the z axis, c, according to[20]

$$\lambda_{001} = \frac{2}{3}\frac{1}{c_0}\frac{dE_{\mathrm{MCA}}}{dc} \Big/ \frac{d^2E_{\mathrm{tot}}}{dc^2}. \tag{1}$$

For the convenience of discussions, we remind that the lowest-order contribution of H^{SOC} toward the total energy is

$$E^{sl} = -(\xi)^2 \sum_o \sum_u \frac{|\langle o|\vec{\sigma}\cdot\vec{L}|u\rangle|^2}{\varepsilon_u - \varepsilon_o}, \tag{2}$$

where ξ is the SOC coupling strength constant, and o and u represent the sets of occupied and unoccupied states, respectively. For contributions from the d states, the nonzero matrix elements of the L_z and L_x operators are $\langle xz|L_z|yz\rangle = 1$, $\langle x^2-y^2|L_z|xy\rangle = 2$, $\langle z^2|L_x|xz,yz\rangle = \sqrt{3}$, $\langle xy|L_x|xz,yz\rangle = 1$, and $\langle x^2-y^2|L_x|xz,yz\rangle = 1$.

III. RESULTS AND DISCUSSIONS

It is known that a well-optimized structure is critical for the determination of electronic and magnetic properties. We first determined lattice constants and elastic constants of these structures from total-energy calculations and the results are given in Table I. The lattice size shrinks gradually when the concentration of Be increases. This is understandable since the size of Be is much smaller than that of Fe. Quantitatively, the calculated lattice constants for different compositions agree with the experimental data. For the bulk Fe, we obtained $C_{11}=234$ GPa and $C_{12}=136$ GPa, both numbers agreeing excellently with experimental values, $C_{11}=232$ GPa and $C_{12}=136$ GPa.[21] This confirms the accuracy of the present calculations. The elastic constants of $Fe_{1-x}Be_x$ alloys depend on their specific atomic structures. It is interesting that $Fe_{0.8125}Be_{0.1875}$ with the atomic structure in Fig. 1(c) has very small tetragonal shear modulus, $C'=(C_{11}-C_{12})/2=11$ GPa. According to Eq. (1), this should lead to enhancement in magnetostriction of $Fe_{0.8125}Be_{0.1875}$ and more details will be presented later.

We found that the Fe atoms located at the body-centered positions in Fig. 1, denoted as Fe(C) hereafter, have the strongest contribution toward magnetostriction since they are the nearest to Be atoms. The presence of Be substituents effectively reduces the number of nearest Fe neighbors around Fe(C) and hence weakens the Fe-Fe hybridization. As a result, the local spin polarization around Fe(C) is enhanced considerably. As listed in Table I, the spin magnetic moments in the Fe(C) muffin-tin sphere increase to 2.296, 2.375, 2.393, and 2.293 μ_B in $Fe_{0.9375}Be_{0.0625}$, $Fe_{0.875}Be_{0.125}$, $Fe_{0.8125}Be_{0.1875}$, and $Fe_{0.75}Be_{0.25}$, respectively. The magnetic moment for $Fe_{0.8125}Be_{0.1875}$ is the largest among the four configurations. The reduction in magnetization at high Be concentration is caused by the shrinkage of lattice constant. The magnetic moments of the Be atoms are also appreciable, −0.158, −0.182, −0.152, and −0.112 μ_B for $Fe_{0.9375}Be_{0.0625}$, $Fe_{0.875}Be_{0.125}$, $Fe_{0.8125}Be_{0.1875}$, and $Fe_{0.75}Be_{0.25}$, respectively. As a reference, the spin-density contour of $Fe_{0.8125}Be_{0.1875}$ plotted on the (110) plane is shown in Fig. 2. Clearly, the spin polarization is negative around Be and its vicinity and the main feature of the spin density around Fe is not much different from that in the bulk Fe.

For the determination of magnetostrictive coefficients according to Eq. (1), we calculated the strain dependences of total and MCA energies of the $Fe_{1-x}Be_x$ alloys. As a benchmark, the calculated λ_{001} for the bcc bulk Fe from the curvature of E_{tot} and slope of E_{MCA} is 21 ppm, a number which

TABLE I. The calculated lattice constants (a in a.u.), total spin magnetic moments (M_{tot} in μ_B) per Fe atom, spin magnetic moments within the MT sphere of the body-centered Fe ($M_{\mathrm{Fe(C)}}$ in μ_B), spin magnetic moments within the MT sphere of Be (M_{Be} in μ_B), elastic constants (C_{11} and C_{12} in GPa), and magnetostrictive coefficients (λ_{001} in 10^{-6}) of $Fe_{1-x}Be_x$.

x	a	C_{11}	C_{12}	M_{tot}	$M_{\mathrm{Fe(C)}}$	M_{Be}	λ_{001}
0.0	5.410	234	136	2.19	2.24		21
0.0625	5.336	256	142	2.18	2.30	−0.16	−36
0.125	5.331	202	107	2.26	2.38	−0.18	76
0.1875	5.302	186	164	2.27	2.39	−0.15	1060
0.25	5.265	288	189	2.24	2.29	−0.11	160

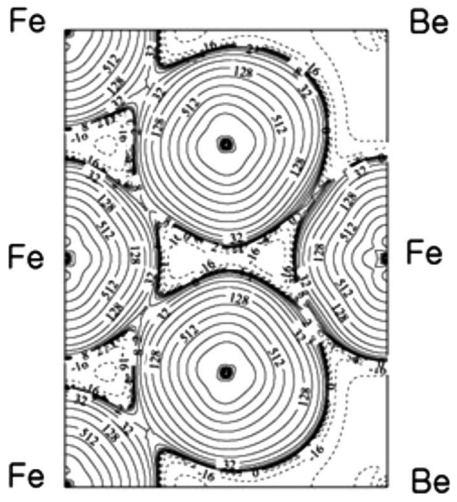

FIG. 2. The spin-density contours of $Fe_{0.8125}Be_{0.1875}$ plotted on the (110) plane. The unit of numbers is e/a.u.^{3}

agrees perfectly with experimental data. As an example for $Fe_{1-x}Be_x$ alloys, Fig. 3 shows the results of $Fe_{0.8125}Be_{0.1875}$. Overall, the data points manifest the quality of our calculations, with E_{tot} and E_{MCA} being fitted nicely by cubic and quadratic lines, respectively. Using Eq. (1), we found that λ_{001}=−36, +76, +1060, and +160 ppm for $Fe_{0.9375}Be_{0.0625}$, $Fe_{0.875}Be_{0.125}$, $Fe_{0.8125}Be_{0.1875}$, and $Fe_{0.75}Be_{0.25}$, in the structures given in Fig. 1. To reflect the uncertainties involved in the fitting procedure, a ±5% error bar should be assigned to these values. It is known that Fe-rich alloys with Ga, Al, and Be have disordered $A2$ phase in equilibrium but local $D0_3$ and $B2$ structures may also form under certain conditions. Therefore, direct comparison with experimental data might need some cautiousness. In particular, we obtained a negative λ_{001} for $Fe_{0.9375}Be_{0.0625}$, a result that is inconsistent with experimental data, ~75 ppm. This discrepancy may indicate the possibility of nonuniform distribution of Be in Fe-Be alloys at low concentration. Calculations with more distribution patterns are underway to address this issue.

Nevertheless, the huge enhancement of λ_{001}, up to +1060 ppm in the selected structure for $Fe_{0.8125}Be_{0.1875}$, is a major finding in the field. This value is much larger than the

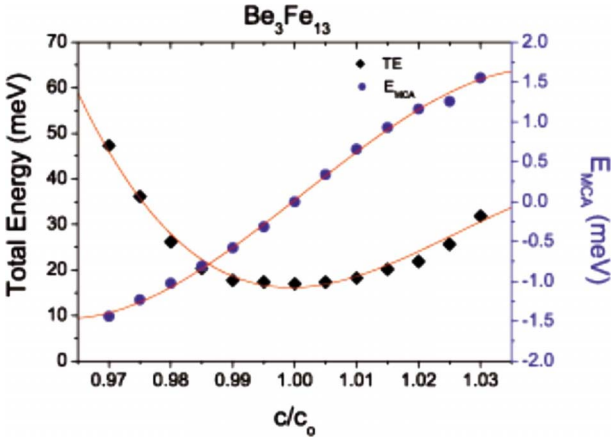

FIG. 3. (Color online) Total energy and MCA energy of $Fe_{0.8125}Be_{0.1875}$ as functions of c/c_0 ratio.

TABLE II. Contributions to E_{MCA} (meV) from spin-orbit couplings between different spin blocks of $Fe_{0.9375}Be_{0.0625}$, $Fe_{0.875}Be_{0.125}$, and $Fe_{0.8125}Be_{0.1875}$ under 2% elongation.

System	c/c_0	DD	UD	UU
$Fe_{0.9375}Be_{0.0625}$	1.02	−0.152	−0.156	0.059
$Fe_{0.875}Be_{0.125}$	1.02	0.312	−0.018	0.024
$Fe_{0.8125}Be_{0.1875}$	1.02	0.988	0.154	0.040

experimental data for the same composition because that the samples may encompass various different phases. Therefore, if one can find means to arrange Be atoms as in Fig. 1(c), much larger magnetostriction is attainable in metallic alloys for practical applications. We want to point out that the calculated λ_{001} of $Fe_{0.8125}Ga_{0.1875}$ with the same structure is −50 ppm. As discussed below, the huge change between Ga-Fe and Be-Fe alloys comes from the difference between their numbers of valence electrons.

To further reveal the governing factor, we focus on $Fe_{0.8125}Be_{0.1875}$ in the discussions below. We first split the contributions from different spin channels by turning on/off SOC in different blocks of the Hamiltonian. As listed in Table II, it is apparent that E^{DD} is dominant compared to E^{UU} and E^{UD}. Here, U (spin-up) and D (spin-down) denote spins of the two states involved in the SOC interaction described in Eq. (2). We also performed separate calculations with H^{SOC} from different atoms and found that Fe(C) atoms provide 90% contributions to the enhancement of λ_{001}. Therefore, we only have to discuss SOC interaction across the Fermi level in the minority-spin channel, for states localized around Fe(C). Figure 4(a) displays the density of states (DOS) of Fe(C), projected onto the e_g and t_{2g} orbitals. For comparison, we also present the corresponding data of the bulk bcc Fe in Fig. 4(b). One can find several remarkable differences between DOS curves of $Fe_{0.8125}Be_{0.1875}$ and the bulk Fe: (i) some nonbonding t_{2g} states shift toward the Fermi level and produce a major peak right above the Fermi energy E_F, and (ii) the e_g band gains occupation because of intra-atomic charge redistribution. Nonetheless, the delicate balance among the e_g and t_{2g} orbitals ensures zero uniaxial E_{MCA}, as required by the symmetry for the undistorted lattices.

To observe how the tetragonal distortion breaks the delicate balance, we first plot the distortion-induced change in DOS $[\Delta\mathrm{DOS}(E)=\mathrm{DOS}(c/c_0=1.03)-\mathrm{DOS}(c/c_0=0.97)]$ of bulk bcc Fe in Fig. 5(a). The lattice expansion (contraction) along the z axis (xy axes) cause major effects: (1) the broadening (narrowing) of unoccupied x^2-y^2 (z^2) d states, along with (2) the upward (downward) shift of the xy (xz,yz) d states right under the Fermi level. According to Eq. (2) and the nonvanishing matrix elements listed right after, these changes weaken the in-plane contributions, through $\langle L_x\rangle$, whereas they enhance the perpendicular contribution, through $\langle L_z\rangle$, toward E_{MCA}. Therefore, the system possesses a positive uniaxial E_{MCA} when the lattice is stretched along the z axis, or vice versa. This explains the positive sign of λ_{001} for the bulk Fe. It is interesting to note the correlation between curves of $\Delta\mathrm{DOS}(E)$ and $E_{MCA}(E)$ [cf. Fig. 5(b)].

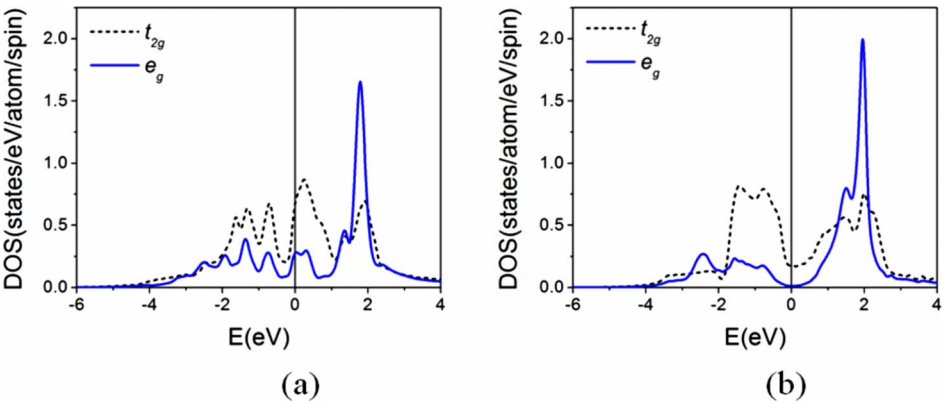

FIG. 4. (Color online) Curves of density of states of minority spin projected into the Fe(C) atom in (a) the $Fe_{0.8125}Be_{0.1875}$ alloy and (b) the bulk Fe at $c/c_0=1$.

Once the Fermi level is placed below the d_{xy} peak in $\Delta\mathrm{DOS}(E)$, $E_{\mathrm{MCA}}(E)$ becomes negative since the $\langle xy|L_z|x^2-y^2\rangle$ term does not provide positive contributes to E_{MCA} any longer as unoccupied states.

In contrast, the origin of the positive magnetostriction coefficient of $Fe_{0.8125}Be_{0.1875}$ is different from that of the bulk Fe. Figure 6(a) presents the strain-induced changes in DOS of the minority spin of Fe(C) in $Fe_{0.8125}Be_{0.1875}$, i.e., the difference of DOS at $c/c_0=1.02$ from DOS at $c/c_0=0.98$ $[\mathrm{DOS}(c/c_0=1.02)-\mathrm{DOS}(c/c_0=0.98)]$. The curves are much more complex compared to those of the bulk Fe displayed in Fig. 5, especially in the range near the Fermi level. It is clear that the lattice elongation affects the xy and xz,yz d states differently. One can see that the d_{xy} state loses electrons to the $d_{xz,yz}$ states when the lattice is stretched along the z axis. Similar charge transfer also occurs from the d_{z^2} state to the $d_{x^2-y^2}$ state. In fact, the opposite changes for the two pairs are seen over the entire energy range. The concurrence of the occupied $d_{x^2-y^2}$ state and unoccupied d_{xy} state around the Fermi level gives large positive contribution to E_{MCA}, through matrix element of $\langle x^2-y^2|L_z|xy\rangle$. Meanwhile, the negative contribution from $\langle z^2|L_x|xz,yz\rangle$ is weakened since the $d_{xz,yz}$ is partially shifted to the occupied region but no obvious increase in the d_{z^2} state in the unoccupied region.

To manipulate magnetostriction, it is instructive to study the band filling dependence of E_{MCA} for positive and negative strains. The calculated E_{MCA} of $Fe_{0.8125}Be_{0.1875}$ at $c/c_0=1.02$ and 0.98 are given as a function of band filling in Fig. 6(b), denoted by the energy shift away from the real Fermi level. It is interesting to note that the real Fermi level sits right at the peak position of the $E_{\mathrm{MCA}}(E)$ curve and thus any change in the number of electrons decreases λ_{001}. This explains why $Fe_{0.8125}Ga_{0.1875}$ in the same structure has a small negative magnetostriction as aforementioned. As shown in Fig. 6(b), Ga atom has one more valence electron than Be atom and hence the Fermi-level shift to the position of the dotted line. Obviously, λ_{001} become small and negative as we obtained from full calculations for $Fe_{0.8125}Ga_{0.1875}$.

IV. CONCLUSIONS

We investigated magnetostrictive behaviors of the bulk Fe and $Fe_{1-x}Be_x$ alloys, through the first-principles calculations, with several uniform structures in Fig. 1. We found that the presence of Be atoms weakens Fe-Fe hybridization and moves d states around the Fermi level, in particular for the Fe(C) atom. This drastically strengthens the spin-orbit coupling interaction between occupied and unoccupied states and therefore enhances the magnetic anisotropy energies when the lattice is slightly distorted. The huge increase in λ_{001} of $Fe_{0.8125}Be_{0.1875}$ is explained in terms of single-particle energy spectra. It is demonstrated that density-functional calculations and rigid-band model analysis are useful in predict-

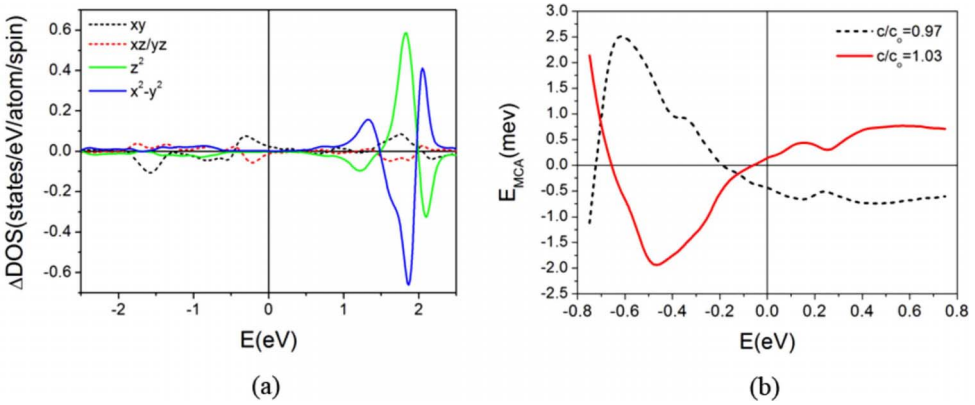

FIG. 5. (Color online) Strain-induced changes in DOS of minority spin of (a) bulk Fe at $c/c_0=1.03$ from $c/c_0=0.97$, $\mathrm{DOS}(c/c_0=1.03)-\mathrm{DOS}(c/c_0=0.97)$, and (b) the calculated E_{MCA} of bulk Fe at $c/c_0=1.03$ (solid line) and 0.97 (dotted line) as a function of the band filling denoted by the energy away from the real Fermi level.

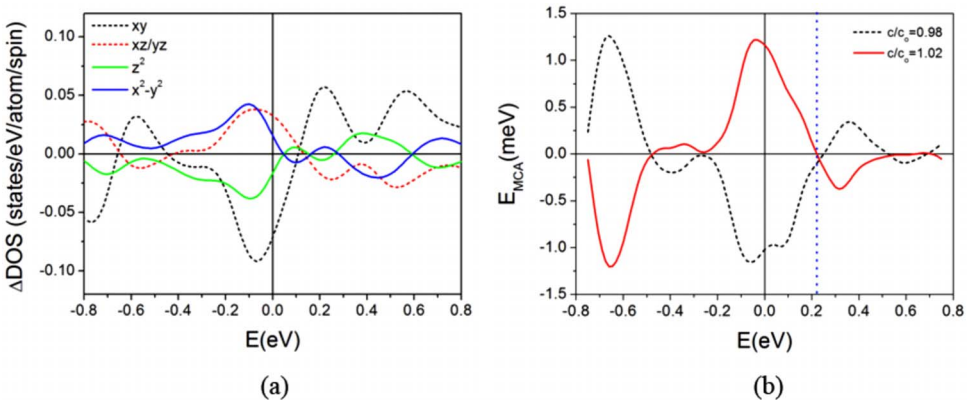

FIG. 6. (Color online) (a) Strain-induced changes in minority-spin DOS of the Fe(C) atom at $c/c_0=1.02$ from $c/c_0=0.98$, DOS($c/c_0=1.02$)−DOS($c/c_0=0.98$), and (b) the calculated E_{MCA} at $c/c_0=1.02$ (solid line) and 0.98 (dotted line) as a function of band filling for the $Fe_{0.8125}Be_{0.1875}$ alloy.

ing and explaining magnetostrictive properties of transition-metal alloys.

ACKNOWLEDGMENTS

We thank A. E. Clark, M. Wun-Fogle, K. B. Hathaway, A. Flatau, and T. Lograsso for simulative discussions. The research in Korea was supported by grants from the Basic Research (Grant No. R01-2007-000-11593-0) and NRL (Grant No. R0A-2006-000-10241-0) Programs of KOSEF. Work in USA was supported by the ONR (Grant No. N00014-08-1-0143) and NSF (Grant No. DMR-0706503). Calculations were performed on supercomputers of NAVO, ARSC, and ERDC.

*schong@mail.ulsan.ac.kr
†wur@uci.edu

[1] A. E. Clark and K. B. Hathaway, in *Handbook of Giant Magnetostrictive Materials*, edited by G. Engdahl (Academic, San Diego, 2002).
[2] R. Q. Wu, in *Modern Trends in Magnetostriction Study and Application*, edited by M. R. J. Gibbs (Kluwer Academic, London, 2001).
[3] A. E. Clark, J. B. Restorff, M. Wun-Fogle, T. A. Lograsso, and D. L. Schlagel, IEEE Trans. Magn. **36**, 3238 (2000).
[4] J. R. Cullen, A. E. Clark, M. Wun-Fogle, J. B. Restorff, and T. A. Lograsso, J. Magn. Magn. Mater. **226-230**, 948 (2001).
[5] R. A. Kellogg, A. B. Flatau, A. E. Clark, M. Wun-Fogle, and T. A. Lograsso, J. Appl. Phys. **91**, 7821 (2002).
[6] A. E. Clark, M. Wun-Fogle, J. B. Restorff, T. A. Lograsso, and G. Petculescu, J. Appl. Phys. **95**, 6942 (2004).
[7] S. Guruswamy, N. Srisukhumbowornchai, A. E. Clark, J. B. Restorff, and M. Wun-Fogle, Scr. Mater. **43**, 239 (2000).
[8] R. Q. Wu and A. J. Freeman, J. Magn. Magn. Mater. **200**, 498 (1999).
[9] R. Q. Wu, J. Appl. Phys. **91**, 7358 (2002).
[10] A. G. Khachaturyan and D. Viehland, Metall. Mater. Trans. A **38**, 2308 (2007).
[11] J. Cullen, P. Zhao, and M. Wuttig, J. Appl. Phys. **101**, 123922 (2007).
[12] T. Khmelevska, S. Khmelevksyi, and P. Mohn, J. Appl. Phys. **103**, 073911 (2008).
[13] A. E. Clark, M. Wun-Fogle, J. B. Restorff, and T. A. Lograsso, IEEE Trans. Magn. **37**, 2678 (2001).
[14] R. Q. Wu, Z. X. Yang, and J. S. Hong, J. Phys.: Condens. Matter **15**, S587 (2003).
[15] G. Petculescu, K. B. Hathaway, T. A. Lograsso, M. Wun-Fogle, and A. E. Clark, J. Appl. Phys. **97**, 10M315 (2005).
[16] A. E. Clark, K. B. Hathaway, M. Wun-Fogle, J. B. Restorff, T. A. Lograsso, V. M. Keppens, G. Petculescu, and R. A. Taylor, J. Appl. Phys. **93**, 8621 (2003).
[17] E. Wimmer, H. Krakauer, M. Weinert, and A. J. Freeman, Phys. Rev. B **24**, 864 (1981).
[18] M. Weinert, E. Wimmer, and A. J. Freeman, Phys. Rev. B **26**, 4571 (1982).
[19] J. P. Perdew, K. Burke, and M. Ernzerhof, Phys. Rev. Lett. **77**, 3865 (1996).
[20] R. Q. Wu, L. J. Chen, A. Shick, and A. J. Freeman, J. Magn. Magn. Mater. **177-181**, 1216 (1998).
[21] C. Kittel, *Introduction to Solid State Physics*, 7th ed. (Wiley, New York, 1996).